BETZEL, C., SAENGER, W., HINGERTY, B. & BROWN, G. (1984). *J. Am. Chem. Soc.* **106**, 7545–7557.
FUJIWARA, T., TOMITA, K., MARSEIGNE, I. & VICENS, J. (1988). *Mol. Cryst. Liq. Cryst. Incl. Nonlinear Opt.* **156**, 393–404.
HAMILTON, J. (1985). *Carbohydr. Res.* **142**, 21–37.
HAMILTON, J. & CHEN, L. (1988*a*). *J. Am. Chem. Soc.* **110**, 4379–4391.
HAMILTON, J. & CHEN, L. (1988*b*). *J. Am. Chem. Soc.* **110**, 5833–5841.
HAMILTON, J. & SABESAN, M. (1982*a*). *Carbohydr. Res.* **102**, 31–46.
HAMILTON, J. & SABESAN, M. (1982*b*). *Acta Cryst.* B**38**, 3063–3069.
HARATA, K. (1982). *Bull. Chem. Soc. Jpn*, **55**, 2315–2320.
HARATA, K. (1984). *Bull. Chem. Soc. Jpn*, **57** (9), 2596–2599.
HARATA, K. (1990). *Minutes International Symposium on Cyclodextrins, Paris*, p. 77. Paris: Editions de Santé.
HARATA, K., UEKAMA, K., OTAGIRI, M., HIRAYAMA, F. & OHTANI, Y. (1985). *Bull. Chem. Soc. Jpn*, **58**(4), 1234–1238.
HARDING, M., MACLENNAN, J. & PATON, M. (1978). *Nature (London)*, **274**, 621–623.
HURSTHOUSE, M., SMITH, C., THORNTON-PETT, M. & UTLEY, J. (1982). *J. Chem. Soc. Chem. Commun*, pp. 881–882.
JOGUN, K. (1979). PhD Thesis, Univ. Stuttgart, Germany.
JOHNSON, C. K. (1976). *ORTEP*II. Report ORNL-5138. Oak Ridge National Laboratory, Tennessee, USA.
KOEHLER, J., SAENGER, W. & VAN GUNSTEREN, W. (1987). *Eur. Biophys. J.* **15**, 211–224.
LE BAS, G. (1985). PhD Thesis, Univ. de Pierre et Marie Curie, Paris, France.
LE BAS, G., RYSANEK, N. & TSOUCARIS, G. (1990). *Minutes International Symposium on Cyclodextrins, Paris*, p. 114. Paris: Editions de Santé.
LE BAS, G. & TSOUCARIS, G. (1986). *Mol. Cryst. Liq. Cryst.* **137**, 287–301.
LINDNER, K. & SAENGER, W. (1982). *Carbohydr. Res.* **99**, 103–115.
MAVRIDIS, I., HADJOUDIS, E. & TSOUCARIS, G. (1990*a*). *Mol. Cryst. Liq. Cryst.* **186**, 185–188.
MAVRIDIS, I., HADJOUDIS, E. & TSOUCARIS, G. (1990*b*). *Minutes International Symposium on Cyclodextrins, Paris*, p. 154. Paris: Editions de Santé.
MENTZAFOS, D., MAVRIDIS, I., LE BAS, G. & DE RANGO, C. (1990). *Minutes International Symposium on Cyclodextrins, Paris*, p. 158. Paris: Editions de Santé.
NAKANISHI, I., ARAI, M., FUJIWARA, T. & TOMITA, K. (1984). *J. Incl. Phenom.* **2**, 689–699.
NAKANISHI, I., FUJIWARA, T. & TOMITA, K. (1984). *Acta Cryst.* A**40**, C-78.
NISHIOKA, F., NAKANISHI, I., FUJIWARA, T. & TOMITA, K. (1984). *J. Incl. Phenom.* **2**, 701–714.
Notes for authors (1983). *Acta Cryst.* A**39**, 174–196.
ONDA, M., YAMAMOTO, Y., INOUE, Y. & CHUJO, R. (1988). *Bull. Chem. Soc. Jpn*, **61**, 4015–4021.
SAENGER, W. (1980). *Angew Chem. Int. Ed. Engl.* **19**, 344–362.
SAENGER, W. (1984). *J. Incl. Phenom.* **2**, 445–454.
SAENGER, W. (1985). *Isr. J. Chem.* **25**, 43–50.
SHELDRICK, G. M. (1976). *SHELX*76. Program for crystal structure determination. Univ. of Cambridge, England.
STEINER, T., HINRICHS, W., SAENGER, W. & HOYER, G.-A. (1989). *Carbohydr. Res.* **192**, 43–49.
STEZOWSKI, J. (1985). *Trans. Am. Crystallogr. Assoc.* pp. 73–82.
STEZOWSKI, J., JOGUN, K., ECKLE, E. & BARTELS, K. (1978). *Nature (London)*, **274**, 617–619.
STODDART, J. F. & ZARZYCKI, R. (1988). *Recl Trav. Chim. Pays-Bas*, **107–109**, 515–528.
TABUSHI, I. & KURODA, Y. (1983). *Adv. Catal.* **32**, 417–466.
TOKUOKA, R., FUJIWARA, T. & TOMITA, K. (1981). *Acta Cryst.* B**37**, 1158–1160.
TSOUCARIS, G., LE BAS, G., RYSANEK, N. & VILLAIN, F. (1987). *J. Incl. Phenom.* **5**, 77–84.
ZABEL, V., SAENGER, W. & MASON, S. (1986). *J. Am. Chem. Soc.* **108**, 3664–3673.

Acta Cryst. (1991). B**47**, 757–766

Phase Transitions in $N(CH_3)_4HSO_4$: a Novel Compound with an Incommensurate Phase

BY NIVALDO L. SPEZIALI† AND GERVAIS CHAPUIS

Université de Lausanne, Institut de Cristallographie, BSP-Dorigny, 1015 *Lausanne, Switzerland*

(*Received* 2 *October* 1990; *accepted* 20 *March* 1991)

Abstract

Two phase transitions have been detected by calorimetric and optical studies in crystals of $N(CH_3)_4HSO_4$. At $T_i = 232$ (2) K, the crystal undergoes a second-order orthorhombic to incommensurate transition and at $T_c = 202$ (2) K, a first-order incommensurate to monoclinic transition. The structures of the three phases have been studied by single-crystal X-ray diffraction. The orthorhombic normal phase, measured at room temperature, exhibits two orientations of the sulfate ions. In the incommensurate phase, the modulation vector is parallel to **c*** with $\mathbf{q} \simeq 0{\cdot}39\mathbf{c}^*$; the two orientations of the sulfate are retained in this phase. The structure of the low-temperature phase was determined at 175 K; the orientational phenomenon disappears while twin domains are observed. Crystal data: tetramethylammonium hydrogen sulfate, $C_4H_{12}N^+.HO_4S^-$, $M_r = 171{\cdot}2$. At room temperature: $Pn2_1a$, $a = 16{\cdot}467$ (9), $b = 7{\cdot}543$ (6), $c = 6{\cdot}939$ (5) Å, $Z = 4$, λ(Mo $K\alpha$) = 0·71069 Å, $R = 0{\cdot}055$ for 931 reflections. At $T = 215$ K: $P^{Pn2_1a}_{11\frac{1}{2}}$, $a = 16{\cdot}230$ (4), $b = 7{\cdot}581$ (2), $c = 6{\cdot}825$ (1) Å, $Z = 4$, λ(Cu $K\alpha$) = 1·5418 Å, $R = 0{\cdot}047$ for 647 main reflections. At $T = 175$ K: $P2_1$, $a = 17{\cdot}451$ (1), $b = 7{\cdot}595$ (1), $c = 13{\cdot}563$ (1) Å, $\beta = 112{\cdot}140$ (2)°, $Z = 8$, λ(Cu $K\alpha$) = 1·5418 Å, $R = 0{\cdot}064$ for 1680 reflections.

† Permanent address: Departamento de Fisica, Universidade Federal de Minas Gerais, 30161 Belo Horizonte, Brazil.

0108-7681/91/050757-10$03.00

1. Introduction

A novel compound which exhibits an incommensurate phase is presented. Tetramethylammonium hydrogen sulfate, $N(CH_3)_4HSO_4$, hereafter referred to as TMSO, shows the sequence of phases normal $\leftrightarrow$ incommensurate $\leftrightarrow$ commensurate with decreasing temperature. This compound is parent to the A_2BX_4 family if A_2 is replaced by the two ions $N(CH_3)_4^+$ and H^+. Taking into consideration the phase-transition sequence, one might be tempted to classify TMSO as the first member of a new subfamily of A_2BX_4 compounds. There is, however, no pseudo-hexagonal axis in the crystal structure, as shown below. Consequently, one of the most important characteristics of the A_2BX_4 compounds is absent.

Crystal growth and the first experimental studies on the physical and chemical properties of TMSO crystals have been reported by Arend (1984). Differential scanning calorimetry (DSC) performed on single crystals revealed a sequence of phases typical of compounds with incommensurate phases, *i.e.* a second-order followed by a first-order phase transition which occur with decreasing temperature. A study of the photon self-diffusion in TMSO crystals has been performed by Blinc, Lahajnar, Zupancič & Arend (1984). From NMR investigations, the authors conclude that TMSO exhibits a superionic phase with high proton conductivity above 450 K. Furthermore, they interpret the room-temperature NMR spectrum as characteristic of rotating $N(CH_3)_4^+$ groups. These results will be discussed in the present work. Ferroelectric properties of TMSO (Sawada, Yamaguchi & Suzuki, 1985) have also been studied and the authors present crystallographic results obtained from Weissenberg photographs recorded at room temperature.

The results on TMSO presented in this work are only partially in agreement with the previous studies mentioned above. There are some points that could not be confirmed; in some cases, remarkable deviations were found and these are discussed in the following paragraphs. Crystallographic studies of the normal, incommensurate and commensurate phases were carried out from the diffracted intensities of the three phases. The structure determination of the normal phase revealed the existence of an orientational disorder which persists in the incommensurate phase. In the low-temperature phase evidence for the existence of twinning domains was found.

2. Crystal preparation and stability

Commercial tetramethylammonium hydrogen sulfate monohydrate (Fluka 87726, purer than 98%) was dissolved in a small amount of water. Adding anhydrous absolute ethanol caused flaky white particles to precipitate. After filtering, the resulting powder was vacuum dried at 373 K. A supersaturated solution was then prepared using absolute methanol. Two different methods of crystal growth were used.

Single crystals of tetramethylammonium hydrogen sulfate were grown from a solution through which a temperature gradient was applied. The convection current induced in the solution guaranteed a uniform composition during the whole growth process (Arend, Perret, Wuest & Kerkoc, 1986). Fig. 1 shows the apparatus developed for this synthesis. Crystals of up to 1 cm^3 can be grown by this method. The composition of the crystal was systematically controlled by chemical analysis and the stoichiometry was always confirmed within 0·5%. For single-crystal analysis, the crystals had to be cut to adequate dimensions (tenths of millimeters). Only one cleavage plane exists and the small fragments obtained had no simple geometrical shape.

A second crystal-growth method was used to obtain naturally grown small crystals. A methanolic solution of the compound was prepared using the procedure described above. Saturation was achieved by adding small amounts of dimethyl ketone which has a lower solubility than methanol. The resulting solution was evaporated very slowly in a temperature controlled chamber; a small Teflon ring was rotated inside the liquid at approximately three turns per minute to ensure homogeneity of the solution. This method yielded perfect and transparent crystals in the form of parallelepipeds. Typical dimensions of the crystals were approximately 0·1 × 0·1 × 3·0 mm. The longer edge is parallel to one of the main axes of the unit cell and coincides with the normal to the cleavage plane.

The quality of the crystals was checked by precession photographs recorded at room temperature

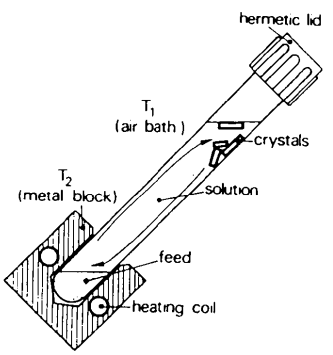

Fig. 1. Apparatus for crystal growth by the convection mechanism due to a temperature difference through the solution. Satisfactory results are obtained with $\Delta T \simeq 2$ or 3 K (according to Arend *et al.*, 1986).

and by the reproducibility of the phase-transition sequence controlled by DSC measurements. Crystals of TMSO are highly hygroscopic: a short exposure to air is sufficient to destroy the crystal and change its properties. For crystallographic measurements, crystals with a volume not exceeding 10^{-2} mm^3 were glued on a glass fiber in a dry argon atmosphere. Much care was taken in order to isolate the crystals from ambient conditions and avoid crystal decomposition during the X-ray diffraction experiments. It should be pointed out that the quality of the crystals used for measurement was optically controlled with a polarizing light microscope; the samples were generally very transparent under polarized light.

3. Thermotropic phase transitions in TMSO

Upon cooling from room temperature, crystals of TMSO undergo two phase transitions: a second-order phase transition at 230 K and a first-order phase transition at 200 K. This sequence was observed by DSC experiments and confirmed by measurements of the optical birefringence (Speziali, 1989; Rivera, Speziali, Berger, Arend & Schmid, 1990). The process is reversible and a small temperature hysteresis was detected. DSC curves are shown in Fig. 2. An additional phase transition appears at 396 K.

The sequence of second- and first-order phase transitions suggests the existence of an incommensurate phase between 230 and 200 K. X-ray diffractograms recorded at room temperature revealed orthorhombic symmetry. Precession photographs below 230 K revealed satellite reflections along an orthorhombic axis. Their positions varied with temperature. Below 200 K, a first-order phase transition induces a change in the lattice parameters and crystal symmetry. The system is monoclinic and the volume of the unit cell is doubled. This leads to the following schematic representation of the phase transition sequence of TMSO:

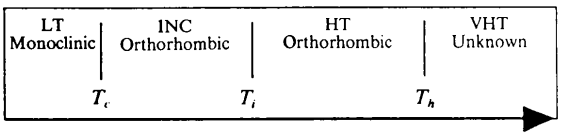

where $T_h = 394$ (2), $T_i = 232$ (2) and $T_c = 202$ (2) K; the values given in parentheses indicate the variation of results between heating and cooling.

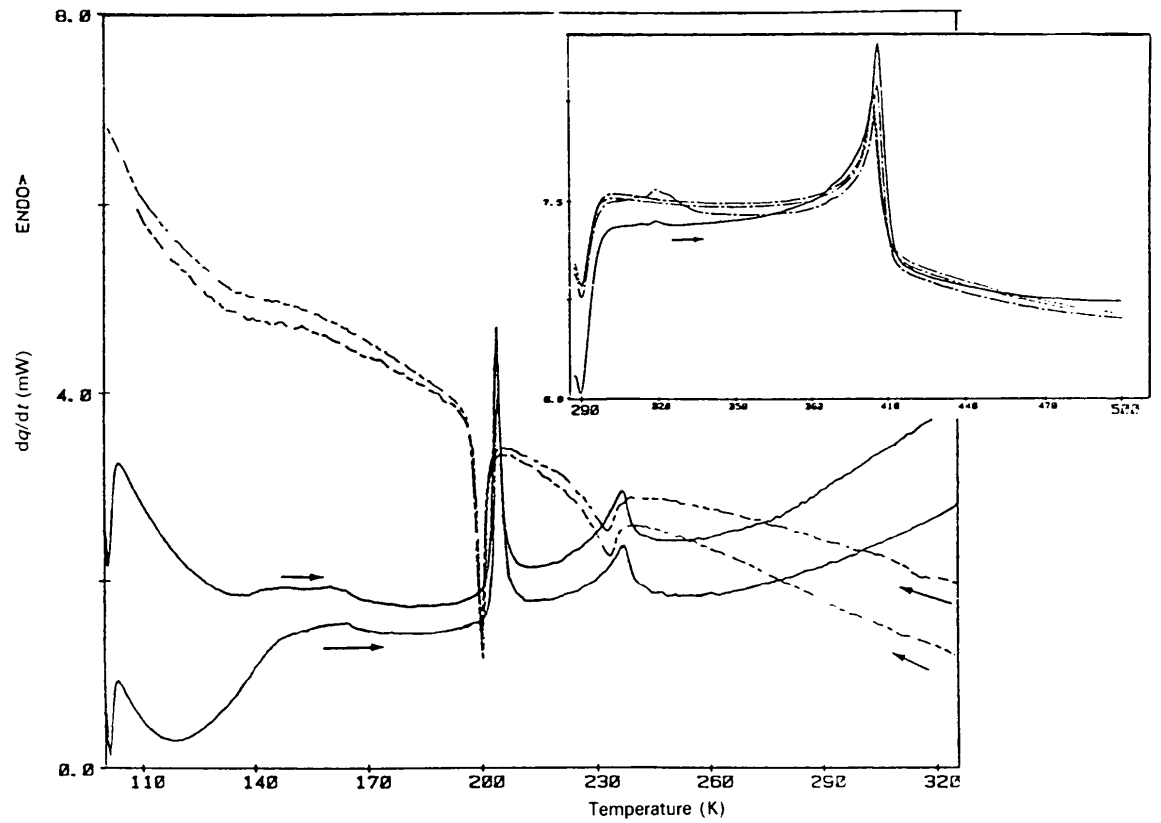

Fig. 2. DSC curves of TMSO crystals. Measurements were performed over two different ranges of temperature; the scan rate was 20 K min^{-1}; the arrows indicate increasing (→) or decreasing (←) temperatures.

Orthoscopic observations of crystal birefringence were performed, in the temperature range from liquid helium to room temperature (Rivera *et al.*, 1990). Measurements were made using a four-order tilting compensator in order to evaluate the range of variation of the difference in the refractive indices. Subsequent measurements using a Babinet–Soleil compensator gave precise values for the phase difference between the two extraordinary beams as a function of temperature. These measurements were performed with a platelet obtained by cleaving a larger crystal perpendicular to **a**. Owing to its hydroscopic character, it was not possible to polish the sample. The faces were not exactly parallel and the width of the plate varied from 0·100 to 0·120 mm. Two phase transitions can be identified on the birefringence curve (Fig. 3). A clear discontinuity in Δn is observed at $T_c = 202$ K which is characteristic of a first-order phase transition. An inflection point at $T_i = 232$ K indicates a continous variation in Δn. The temperature hysteresis (0·6 K) for the first-order phase transition was deduced from these measurements. The rate of temperature variation was 1·5 K min^{-1} during the experiment.

Temperatures reported in this work are calibrated with respect to DSC values. With X-ray diffraction, the temperature at the crystal differs slightly from the thermocouple values.

4. Orthorhombic normal (HT) phase

4.1. *Structure determination*

Analysis of X-ray diffraction intensities from five different samples (grown and prepared by different methods) yielded the same structural results. The disorder found at room temperature seems to be intrinsic to TMSO. The results reported here represent the best set of measurements on a single crystal with:

(i) the largest number of equivalent reflections and $\sin\theta/\lambda$,

(ii) the lowest scan speed during ω–2θ measurement,

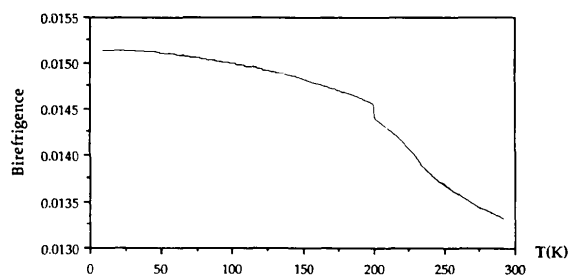

Fig. 3. Birefringence measurements of TMSO crystals in the temperature range from liquid helium to room temperature.

Table 1. *Data collection and data reduction characteristics for the room-temperature (HT) phase*

Scan mode	ω–2θ
Scan width (°)	$1{\cdot}0 + 0{\cdot}35\tan\theta$
Scan speed (° min^{-1})	1·50 to 9·77
$(\sin\theta/\lambda)_{max}$ (Å^{-1})	0·597
Range of hkl	$-16 \le h \le 16$, $-8 \le k \le 8$, $0 \le l \le 8$
No. of reflections measured	4188
No. of unique reflections	931
No. of observed reflections	566 [$I_o \ge 3\sigma(I_o)$]
Internal consistency R_{int}	0·0189

Table 2. *Fractional atomic coordinates and population parameters (p) for space group $Pn2_1a$ (e.s.d.'s in parentheses)*

	x	y	z	p
S	0·08563 (8)	0·2539 (6)	0·0656 (2)	
O(1)	0·1254 (6)	0·289 (2)	0·247 (1)	0·450 (9)
O(2)	0·1271 (7)	0·329 (2)	−0·095 (1)	0·450
O(3)	0·0009 (4)	0·340 (1)	0·078 (2)	0·450
O(4)	0·0713 (7)	0·0634 (7)	0·040 (2)	0·450
O(11)	0·1509 (4)	0·214 (1)	0·193 (1)	0·550
O(21)	0·1084 (4)	0·254 (2)	−0·1346 (8)	0·550
O(31)	0·0536 (6)	0·4392 (7)	0·115 (2)	0·550
O(41)	0·0162 (5)	0·1324 (9)	0·098 (2)	0·550
N	0·3634 (2)	0·256 (2)	−0·0261 (7)	
C(1)	0·4522 (3)	0·266 (3)	−0·068 (1)	
C(2)	0·3178 (4)	0·251 (3)	−0·213 (1)	
C(3)	0·3470 (8)	0·091 (2)	0·084 (2)	
C(4)	0·3391 (9)	0·412 (2)	0·080 (2)	

(iii) the best stability of periodically checked control reflections.

The internal consistency of equivalent reflections ($R_{int} = 0{\cdot}0189$) confirmed the quality of the data (98·3% of the reflections were measured more than once). Preliminary precession and Weissenberg diffractograms indicated orthorhombic symmetry and the following extinction rules:

$$h = 2n + 1 \quad \text{for } hk0 \qquad (1a)$$

$$k + l = 2n + l \quad \text{for } 0kl. \qquad (1b)$$

X-ray intensities were collected on a Syntex $P2_1$ four-circle diffractometer using the ω–2θ-scan technique and Mo $K\alpha$ radiation. The lattice parameters were determined by a least-squares fit of 15 accurately centered reflections giving $a = 16{\cdot}467$ (9), $b = 7{\cdot}543$ (6) and $c = 6{\cdot}939$ (5) Å. Owing to the hygroscopic character of the TMSO crystals, their density was calculated by measuring directly the volume and the mass of a large sample. The value found ($D_m = 1{\cdot}35$ g cm^{-3}) agrees with the lattice constants for $Z = 4$ ($D_x = 1{\cdot}32$ g cm^{-3}). The extinction conditions were confirmed on the diffractometer except for the reflection (010) with an intensity ten times larger than its e.s.d. This was due to an harmonic effect of the very strong (020) reflection. Since the X-ray absorption coefficient of TMSO is small, $\mu_{Mo\,K\alpha} = 3{\cdot}38$ cm^{-1}, the correction could be neglected. Lorentz and polarization corrections were accounted for.

Table 3. *Components of displacement tensor* U_{ij} (Å^2) *refined in space group* $Pn2_1a$ *(e.s.d.'s in parentheses)*

	U_{11}	U_{22}	U_{33}	U_{12}	U_{13}	U_{23}
S	0·0513 (7)	0·0467 (7)	0·065 (1)	0·007 (2)	0·001 (1)	−0·005 (2)
O(1)	0·103 (3)	0·133 (3)	0·085 (3)	−0·027 (3)	−0·052 (3)	0·003 (3)
O(2)	0·121 (3)	0·177 (3)	0·107 (3)	0·010 (3)	0·062 (3)	0·060 (3)
O(3)	0·047 (3)	0·072 (3)	0·112 (3)	0·003 (3)	0·003 (3)	0·003 (3)
O(4)	0·068 (3)	0·061 (3)	0·225 (3)	−0·007 (3)	−0·014 (3)	−0·035 (3)
O(11)	0·085 (3)	0·132 (3)	0·114 (3)	0·019 (3)	−0·020 (3)	0·031 (3)
O(21)	0·073 (3)	0·081 (3)	0·069 (3)	−0·046 (3)	0·022 (2)	−0·030 (3)
O(31)	0·088 (3)	0·060 (3)	0·113 (3)	0·004 (2)	−0·014 (3)	−0·051 (3)
O(41)	0·086 (3)	0·078 (3)	0·104 (3)	−0·044 (3)	0·061 (3)	−0·041 (3)
N	0·051 (2)	0·062 (2)	0·064 (2)	−0·023 (3)	0·002 (2)	−0·025 (3)
C(1)	0·045 (2)	0·134 (3)	0·076 (3)	0·006 (3)	0·001 (2)	0·028 (3)
C(2)	0·064 (2)	0·098 (3)	0·079 (3)	−0·022 (3)	−0·019 (2)	0·006 (3)
C(3)	0·080 (3)	0·082 (3)	0·139 (3)	−0·007 (3)	−0·004 (3)	0·025 (3)
C(4)	0·114 (3)	0·083 (3)	0·112 (3)	−0·011 (3)	0·040 (3)	−0·058 (3)

A summary of the data collection parameters and results is given in Table 1.*

The structure was refined in the polar space group $Pn2_1a$. Two superimposed sulfate ions were found with a common S atom. Site occupations p_1 and p_2 were assigned to each group with the condition $p_1 + p_2 = 1$. The tetramethylammonium ion was well defined. The structure converged to $R = 0{\cdot}055$ and $wR = 0{\cdot}049$, $w = 1/\sigma^2_{F_{obs}}$, including the H atoms. The geometry of the sulfate and the methyl group were restricted in the refinement (Didisheim & Schwarzenbach, 1987). $\Delta/\sigma = 0{\cdot}5$. Atomic scattering factors for C, N, O and S were calculated from Cromer & Mann (1968) and from Stewart, Davidson & Simpson (1965) for H. A local set of computer programs compatible with the *XRAY*72 system (Stewart, Kundell & Baldwin, 1972) and *REMOS*85.0 (Yamamoto, 1982) were used for the refinements. Refined parameters are given in Tables 2 and 3. Table 4 lists the interatomic distances and angles. A projection of the structure is represented along **c** (Johnson, 1965) in Fig. 4. The superposition of the SO_4 tetrahedra results from the orientational disorder.

* Lists of structure factors have been deposited with the British Library Document Supply Centre as Supplementary Publication No. SUP 54094 (23 pp.). Copies may be obtained through The Technical Editor, International Union of Crystallography, 5 Abbey Square, Chester CH1 2HU, England.

Table 4. *Interatomic distances* (Å) *and angles* (°) *in the* $N(CH_3)_4$ *and* SO_4 *tetrahedra for the normal (HT) phase of TMSO*

The O—O distances and O—S—O angles were restrained.

S—O(1)	1·444	O(1)—S—O(2)	113·09
S—O(2)	1·426	O(1)—S—O(3)	106·62
S—O(3)	1·541	O(1)—S—O(4)	110·90
S—O(4)	1·467	O(2)—S—O(3)	107·90
		O(2)—S—O(4)	111·96
		O(3)—S—O(4)	105·92
S—O(11)	1·422	O(11)—S—O(21)	113·65
S—O(21)	1·439	O(11)—S—O(31)	108·35
S—O(31)	1·533	O(11)—S—O(41)	110·87
S—O(41)	1·483	O(21)—S—O(31)	107·78
		O(21)—S—O(41)	110·50
		O(31)—S—O(41)	105·27
N—C(1)	1·493	C(1)—N—C(2)	108·82
N—C(2)	1·497	C(1)—N—C(3)	108·83
N—C(3)	1·482	C(1)—N—C(4)	109·16
N—C(4)	1·450	C(2)—N—C(3)	109·53
		C(2)—N—C(4)	108·71
		C(3)—N—C(4)	111·75

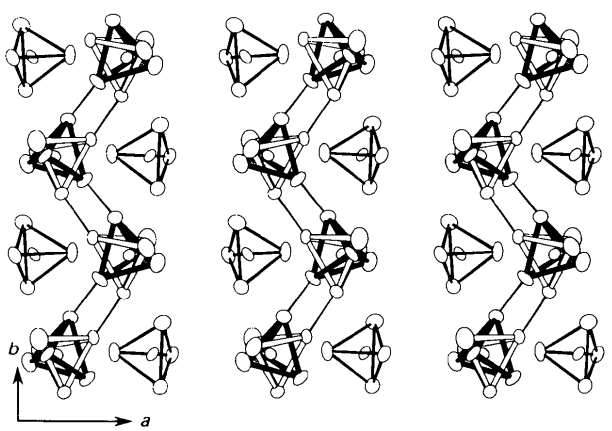

Fig. 4. Projection along [001] of the structure of the HT phase of TMSO. The two orientations of the sulfate chains are represented by superimposed tetrahedra. SO_4 tetrahedra interact with each other *via* hydrogen bonds forming chains in the **b** direction.

4.2. *Discussion of the structure*

The short O···O distances varying from 2·50 to 2·54 Å between sulfate groups clearly indicate the position of the H atom within the structure. No attempts were made, however, to locate the proton. The sulfate ions are thus linked by hydrogen bonds to form chains extending along **b** (Fig. 4). Two types of chain can be identified which are nearly symmetric with respect to a mirror plane normal to **b**. Remembering the superionic character of this compound, it might be inferred that the structure consists of alternating domains which are each characterized by a specific orientation of the SO_4 tetrahedra. The

interface between domains could be due to the absence of hydrogen bonding.

The probability, p_1, of finding a specific SO_4 orientation depends on the crystal specimen. This refinement yielded the value $p_1 = 0{\cdot}45$ (1). The choice of the polar space group $Pn2_1a$ has been confirmed independently by various refinements.

The tetramethylammonium group is well defined. This has been confirmed by refinements on different specimens. This is at variance with the results presented by Blinc *et al.* (1984). The $N(CH_3)_4$ tetrahedra lie on a pseudo-mirror plane normal to **b** and do not contribute significantly to the polarity of the space group.

Some of the crystal-growth experiments resulted in crystals of very inferior quality; yet they revealed some very surprising properties of the TMSO system. In an attempt to grow crystals by means of the evaporation method, a set of polyhedral crystals with many faces were obtained. Under polarized light, no darkening was found. Such a sample was mounted on the four-circle diffractometer to evaluate the lattice parameters and symmetry. Three lattice constants of approximately 9·8 Å ($\simeq c_{orth}2^{1/2}$) and angles of approximately 90° were found. However, diffractograms confirmed that the sample was not a single crystal. Multidomain crystals can be obtained during crystal growth. Sawada *et al.* (1985) reported similar results and one might suspect that they did not deal with single crystals. As stated by those authors, the crystals were prepared by the evaporation of an aqueous solution of $N(CH_3)_4OH{:}H_2SO_4$, in a ratio of 1:1. It should be pointed out that no hygroscopic behavior was reported for their crystals.

5. Incommensurate (INC) phase

With decreasing temperature, crystals of TMSO undergo a second-order phase transition at $T_i = 230$ K. At 220 K, precession photographs revealed the presence of weak satellite reflections along **c*** and $\mathbf{q} \simeq 0{\cdot}39\mathbf{c}^*$. A single crystal with a prismatic habit was mounted on a four-circle diffractometer. Lattice constants and the modulation vector were measured at various temperatures ranging from 200 to 235 K. The crystal was cooled by a stream of nitrogen gas (modified Enraf–Nonius system). For each temperature, a group of 15 reflections was accurately centered and the lattice parameters calculated by least squares. The value of **q** could be precisely measured from three automatically centered satellite reflections. The observed variation of **q** can be expressed by the ratio:

$$|\Delta\mathbf{q}|/\mathbf{q}_{mean} \simeq 14\%$$

with $\mathbf{q}_{mean} = (\mathbf{q}_{min} + \mathbf{q}_{max})/2$. The modulation wavelength is thus strongly dependent on the temperature.

A small temperature variation for the intensities of satellite and main reflections was observed. At 215·0 (3) K, the value of **q** determined from three centered satellite reflections was 0·4183 (4) with the lattice constants $a = 16{\cdot}230$ (4), $b = 7{\cdot}581$ (2) and $c = 6{\cdot}825$ (1) Å. The systematic absences observed for the main reflections were identical to the room-temperature phase. For the average structure, the space-group symmetry is the same as for the normal phase since **q** is parallel to one of the orthorhombic axes (Simmons & Heine, 1987). As a consequence, the (3 + 1)-dimensional superspace group must be $P^{Pn2_1a}_{1\,1\,1}$ (de Wolff, Janssen & Janner, 1981). Analysis of the intensities confirmed the systematic absences of the superspace group. The refinement of the averaged structure including the H atoms converged to $R = 0{\cdot}047$ ($wR = 0{\cdot}043$). The twofold orientation of the SO_4 tetrahedra persists in the INC phase. The determination of the modulated structure will be published elsewhere.

6. Commensurate (LT) phase

6.1. *Symmetry and lattice constants*

On cooling, TMSO crystals undergo a first-order phase transition at $T_c = 200$ K and the symmetry becomes monoclinic with the unique c axis twice that of the normal phase. The phase transition was detected by the disappearance of the satellite reflections. An analysis of some profiles revealed a splitting of the reflections below the transition temperature (Fig. 5). The splitting was completely reversible.

The lattice constants, determined by centering 15 reflections at $T = 175$ K were $a = 17{\cdot}451$ (1), $b = 7{\cdot}595$ (1) and $c = 13{\cdot}563$ (1) Å with $\beta = 112{\cdot}140$ (2)°. The relations of the cell constants (Table 5) can be expressed by:

$$\mathbf{a}_{mon} \simeq \mathbf{a}_{orth} - \mathbf{c}_{orth} \qquad \mathbf{c}_{mon} \simeq 2\mathbf{c}_{orth}$$
$$\mathbf{b}_{mon} \simeq \mathbf{b}_{orth} \qquad V_{mon} \simeq 2V_{orth}.$$

Analysis of the intensities collected on the four-circle diffractometer revealed the following extinction rule:

$$k = 2n + 1 \quad \text{for } 0k0. \qquad (2)$$

The space-group symmetry is thus either $P\,1\,2_1\,1$ or $P\,1\,2_1/m\,1$.

6.2. *Twinning*

The splitting of several reflections observed below T_c is due to the appearance of twinned domains associated with the phase transition. Systematic analyses of a large number of profiles revealed the following observations:

(i) reflections $hk0$ are well behaved,

Table 5. *Lattice constants of the monoclinic phase as a function of temperature*

β' is the angle between $\mathbf{c}_{mon}$ and $2\mathbf{a} - \mathbf{c}_{mon}$.

T (K)	a (Å)	b (Å)	c (Å)	β (°)	β' (°)
195	17·497 (5)	7·592 (2)	13·594 (4)	112·29 (1)	89·43
175	17·451 (1)	7·595 (1)	13·563 (1)	112·14 (1)	89·27
165	17·432 (6)	7·595 (2)	13·556 (4)	112·07 (1)	89·19
150	17·395 (6)	7·595 (2)	13·553 (4)	111·99 (1)	89·01

(ii) in the series (hkl), $(2h,2k,2l)$, $(3h,3k,3l)$... the splitting increases with the Bragg angle,

(iii) reflections measured with various azimuthal angles showed different profiles.

Based on these observations, the domains shown in Fig. 6 are related by a mirror plane perpendicular to **a***. The reciprocal lattice point hkl from one domain nearly coincides with the point $h'k'l'$ from the other domain. The indices are related by the twinning operation:

$$(h',k',l') = (h,k,l)\begin{pmatrix} \bar{1} & 0 & 0 \\ 0 & 1 & 0 \\ \bar{1} & 0 & 1 \end{pmatrix} = (\bar{h} + \bar{l},k,l). \qquad (3)$$

A flat specimen was examined under a polarizing microscope from room down to liquid helium temperature. At $T = T_c$, a sudden appearance of a domain structure was observed. By warming the crystal above T_c the domains disappeared. This indicates the reversibility of the process. Repeating this procedure several times, *i.e.* allowing the first-order transition to take place repeatedly, a phenomenon of fatigue was noticed: some of the domain walls remained at temperatures above T_c indicating that the sample was fissured (Rivera *et al.*, 1990).

6.3. *Data collection*

The ω-scan mode was chosen to collect the data and each reflection was measured for three different values of ψ ($= -10, 0, 10°$) to test the overlap. With this method, a total of 5138 reflections were measured which yielded 1682 unique reflections. 1378 reflections were considered as observed $[I \geq 2\sigma(I)]$ giving $R_{int} = 0{\cdot}039$. A Lorentz–polarization correction was made, but no absorption correction was applied. Table 6 summarizes the conditions for data collection and reduction.

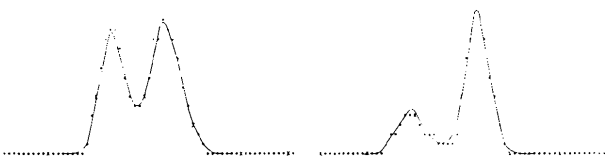

Fig. 5. Splitting of the ω–2θ scan profiles observed in the LT phase of TMSO. In the left profile, the intensities of the two peaks are almost the same; in the sample used for the data collection (right profile), a clear difference is observed between the components.

Table 6. *Data collection and data reduction characteristics for the monoclinic commensurate (LT) phase*

Scan mode	ω (with $\psi = -10,0,10°$)
Scan width (°)	1·60
Scan speed (° min^{-1})	0·60 to 9·77
$(\sin\theta/\lambda)_{max}$ (Å^{-1})	0·478
Range of hkl	$-16 \leq h \leq 16$, $0 \leq k \leq 8$, $-12 \leq l \leq 12$
No. of reflections measured	5138
No. of unique reflections	1680
No. of observed reflections	1376 $[I_o \geq 2\sigma(I_o)]$
Internal consistency R_{int}	0·0390

6.4. *Structure determination*

Restraints on distances and angles (Didisheim & Schwarzenbach, 1987) were imposed on the SO_4 and CH_3 units for the refinement. With the fractional volume parameters, v_1 and v_2, of the twins and the condition $v_1 + v_2 = 1$, the refinement converged to $R = 0{\cdot}064$ with $v_1:v_2 = 0{\cdot}85\,(2):0{\cdot}15$. $\Delta/\sigma = 0{\cdot}2$. The final positional parameters and equivalent displacement coefficients are shown in Table 7; the interatomic distances and angles are given in Table 8. The values of the restrained quantities in each SO_4 tetrahedron were 2·40 Å for the O—O distances (weight = 1/0·003) and 109° for the O—S—O angles (weight = 1/0·175). The computer programs mentioned in §4.1. were used in the refinements.

6.5. *Discussion of the structure*

Below T_c, the superposition of the SO_4 tetrahedra disappears and the existence of twin domains is

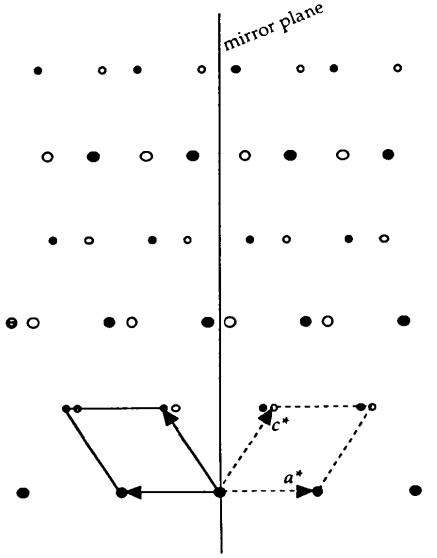

Fig. 6. Superposition of reciprocal lattices of two twin domains. The dashed-line unit cell generates the solid-line unit cell by a reflection through a plane perpendicular to **a***.

Table 7. *Fractional atomic coordinates and equivalent displacement factors* U_{eq} ($Å^2$) *for the monoclinic phase (e.s.d.'s in parentheses)*

Distance and angle constraints were applied.

	x	y	z	U_{eq}
S(1)	0·0840 (3)	0·2539	0·2562 (5)	0·025 (2)
O(11)	0·1165 (9)	0·229 (2)	0·368 (1)	0·048 (2)
O(12)	0·1386 (9)	0·197 (2)	0·205 (1)	0·056 (2)
O(13)	0·0035 (8)	0·151 (2)	0·210 (1)	0·042 (2)
O(14)	0·063 (1)	0·444 (2)	0·230 (1)	0·057 (2)
S(2)	0·4153 (3)	0·7530 (8)	0·6754 (5)	0·023 (2)
O(21)	0·3881 (8)	0·761 (2)	0·761 (1)	0·036 (2)
O(22)	0·3518 (9)	0·802 (2)	0·574 (1)	0·061 (2)
O(23)	0·4432 (9)	0·569 (2)	0·666 (1)	0·044 (2)
O(24)	0·4894 (8)	0·872 (2)	0·697 (1)	0·054 (2)
S(3)	−0·0866 (3)	−0·2506 (8)	0·2426 (5)	0·027 (2)
O(31)	−0·1171 (9)	−0·237 (2)	0·131 (1)	0·043 (2)
O(32)	−0·1441 (8)	−0·207 (2)	0·289 (1)	0·045 (2)
O(33)	−0·0094 (8)	−0·140 (2)	0·290 (1)	0·053 (2)
O(34)	0·0590 (9)	−0·442 (2)	0·274 (1)	0·036 (2)
O(41)	0·3803 (9)	−0·277 (2)	0·253 (1)	0·050 (2)
O(42)	0·3608 (9)	−0·291 (2)	0·070 (1)	0·053 (2)
O(43)	0·4353 (9)	−0·050 (2)	0·175 (1)	0·055 (2)
O(44)	0·4959 (8)	−0·342 (2)	0·204 (1)	0·038 (2)
N(1)	0·3647 (9)	0·239 (2)	0·449 (1)	0·024 (2)
C(11)	0·352 (1)	0·416 (3)	0·390 (2)	0·046 (2)
C(12)	0·457 (1)	0·219 (3)	0·518 (2)	0·029 (2)
C(13)	0·317 (1)	0·237 (3)	0·518 (2)	0·034 (2)
C(14)	0·339 (1)	0·089 (3)	0·371 (2)	0·046 (2)
N(2)	0·1350 (9)	0·732 (2)	0·581 (1)	0·034 (2)
C(21)	0·044 (1)	0·706 (3)	0·560 (2)	0·031 (2)
C(22)	0·182 (1)	0·730 (3)	0·696 (2)	0·031 (2)
C(23)	0·163 (1)	0·589 (3)	0·530 (2)	0·037 (2)
C(24)	0·147 (1)	0·909 (3)	0·535 (2)	0·041 (2)
N(3)	0·3653 (9)	−0·742 (2)	−0·050 (1)	0·034 (2)
C(31)	0·342 (1)	−0·915 (3)	−0·106 (2)	0·033 (2)
C(32)	0·456 (1)	−0·742 (3)	0·014 (2)	0·044 (2)
C(33)	0·320 (1)	−0·716 (3)	0·023 (2)	0·040 (2)
C(34)	0·346 (1)	−0·597 (4)	−0·130 (2)	0·049 (2)
N(4)	0·1346 (9)	−0·241 (2)	0·081 (1)	0·026 (2)
C(41)	0·044 (1)	0·233 (3)	0·058 (2)	0·033 (2)
C(42)	0·181 (1)	−0·215 (3)	0·198 (2)	0·040 (2)
C(43)	0·156 (1)	−0·099 (4)	0·020 (2)	0·046 (2)
C(44)	0·156 (1)	−0·423 (3)	0·048 (2)	0·040 (2)

Table 8. *Interatomic distances* (Å) *and angles* (°) *in the* $N(CH_3)_4$ *and* SO_4 *tetrahedra for the monoclinic phase of TMSO*

S(1)—O(11)	1·423	O(11)—S(1)—O(12)	114·22
S(1)—O(12)	1·442	O(11)—S(1)—O(13)	108·03
S(1)—O(13)	1·521	O(11)—S(1)—O(14)	110·15
S(1)—O(14)	1·497	O(12)—S(1)—O(13)	108·71
		O(12)—S(1)—O(14)	108·79
		O(13)—S(1)—O(14)	106·65
S(2)—O(21)	1·414	O(21)—S(2)—O(22)	113·46
S(2)—O(22)	1·457	O(21)—S(2)—O(23)	109·54
S(2)—O(23)	1·501	O(21)—S(2)—O(24)	109·80
S(2)—O(24)	1·511	O(22)—S(2)—O(23)	107·93
		O(22)—S(2)—O(24)	108·95
		O(23)—S(2)—O(24)	106·95
S(3)—O(31)	1·409	O(31)—S(3)—O(32)	114·91
S(3)—O(32)	1·412	O(31)—S(3)—O(33)	109·50
S(3)—O(33)	1·512	O(31)—S(3)—O(34)	108·85
S(3)—O(34)	1·541	O(32)—S(3)—O(33)	110·22
		O(32)—S(3)—O(34)	107·20
		O(33)—S(3)—O(34)	105·73
S(4)—O(41)	1·417	O(41)—S(4)—O(42)	114·50
S(4)—O(42)	1·414	O(41)—S(4)—O(43)	109·84
S(4)—O(43)	1·525	O(41)—S(4)—O(44)	108·80
S(4)—O(44)	1·531	O(42)—S(4)—O(43)	108·31
		O(42)—S(4)—O(44)	109·71
		O(43)—S(4)—O(44)	105·29
N(1)—C(11)	1·534	C(11)—N(1)—C(12)	108·84
N(1)—C(12)	1·528	C(11)—N(1)—C(13)	109·42
N(1)—C(13)	1·469	C(11)—N(1)—C(14)	110·45
N(1)—C(14)	1·505	C(12)—N(1)—C(13)	108·94
		C(12)—N(1)—C(14)	108·71
		C(13)—N(1)—C(14)	110·44
N(2)—C(21)	1·514	C(21)—N(2)—C(22)	108·79
N(2)—C(22)	1·461	C(21)—N(2)—C(23)	108·79
N(2)—C(23)	1·467	C(21)—N(2)—C(24)	109·47
N(2)—C(24)	1·528	C(22)—N(2)—C(23)	110·21
		C(22)—N(2)—C(24)	109·97
		C(23)—N(2)—C(24)	109·58
N(3)—C(31)	1·499	C(31)—N(3)—C(32)	108·99
N(3)—C(32)	1·489	C(31)—N(3)—C(33)	109·98
N(3)—C(33)	1·494	C(31)—N(3)—C(34)	109·12
N(3)—C(34)	1·498	C(32)—N(3)—C(33)	109·04
		C(32)—N(3)—C(34)	109·14
		C(33)—N(3)—C(34)	110·54
N(4)—C(41)	1·495	C(41)—N(4)—C(42)	108·49
N(4)—C(42)	1·501	C(41)—N(4)—C(43)	109·10
N(4)—C(43)	1·496	C(41)—N(4)—C(44)	109·40
N(4)—C(44)	1·539	C(42)—N(4)—C(43)	110·32
		C(42)—N(4)—C(44)	109·69
		C(43)—N(4)—C(44)	109·82

observed. A projection of the structure onto the **ac** plane is shown in Fig. 7. A comparison of the LT (monoclinic, ordered) phase and the HT (orthorhombic, disordered) phase shows that the two orientations of the SO_4 tetrahedra observed in the HT phase are found in LT with minor differences. Consecutive SO_4 tetrahedra interacting by a hydrogen bond are symmetry independent. The atoms in the $N(CH_3)_4$ groups have approximately the same positions in both phases. The final R factor obtained is rather high. The existence of twin domains might explain some difficulties in the refinement, particularly since it is not a merohedry twinning. A second difficulty arises from the number of refined variables and the number of unique reflections collected, *i.e.* 506 and 1682 respectively.

7. Concluding remarks

The sequence of phase transitions for TMSO has been studied by DSC from room to liquid nitrogen temperature and by optical methods from room to liquid helium temperature. Two phase transitions have been observed. Crystal structures of the three different phases have been determined. The results are summarized in the following scheme:

HT Orthorhombic $\xleftrightarrow{T_i}$ 232(2) K INC Orthorhombic $\xleftrightarrow{T_c}$ 202(2) K LT Monoclinic

$Pn2_1a$ $P^{Pn2_1a}_{11\bar{1}}$ $P12_11$

From the DSC curves and from the birefringence measurements (Figs. 2 and 3) it is evident that the TMSO crystals undergo a first-order phase transition at T_c. In the neighborhood of T_i, Fig. 3 shows a

continuous variation of the birefringence, while at T_i a change in its derivative can be identified. For this reason and considering the shape of the DSC curve, the phase transition at T_i is second order.

The structure of the HT phase shows a disorder of sulfate tetrahedra which adopt two different orientations. By contrast, no disorder of the tetramethylammonium ions could be detected. The structure of the LT phase can be satisfactorily interpreted as resulting from an ordering of the normal phase.

No complete structural analysis has been performed for the INC phase. Some hints can be given about the modulation by considering the crystal structures of the neighboring phases. The positions of the $N(CH_3)_4$ groups are very similar in the normal and commensurate phases. It is thus reasonable to suppose that they do not contribute significantly to the modulation of the INC phase. In the normal HT phase, the two different orientations of the SO_4 ions give rise to two opposite orientations in the commensurate LT phase. They probably have antiphase rotational displacements in the INC phase. Moreover, owing to the temperature dependence of the lattice constants, the existence of a displacement in the **b** direction is probable. An initial model to solve the incommenusurately modulated phase should contain a rotation of the sulfate groups about the **a** direction in addition to a translation in the **b** direction. Both rotational and translational displacements of the tetrahedra, corresponding to the two different orientations, should be half a wavelength out of phase.

Recent studies on superionic properties of TMSO (Blinc *et al.*, 1984) show that the acid protons are responsible for the high ionic conductivity. In the present work, the position of the H^+ ion was not included in the refinements of the TMSO phases. However, from the S—O distances, the O atoms participating in the hydrogen bonds can be clearly identified. The O—H—O distances range from 2·50 to 2·54 Å in the HT phase and from 2·54 to 2·59 Å in the LT phase. These short values agree with an 'acid' hydrogen bond (Hamilton & Ibers, 1968).

It would be of interest to study other similar compounds, $N(CH_3)_4HSeO_4$ for example. The results obtained in the TMSO study, both for crystal preparation and handling, and for structure determination, could be helpful for future analysis of this type of compound. Hydrogen-bonded chains of SO_4 were also observed in $CsHSO_4$ (Itoh, Ozaki & Nakamura, 1981). This compound exhibits a superionic phase with high proton conductivity as well (Baranov, Shuvalov & Shchagina, 1982). It therefore seems that a correlation exists between the proton conductivity and the presence of SO_4 chains in the crystal structure. Another compound with a similar empirical formula, $CsHSeO_4$, also shows a superionic phase (Baranov *et al.*, 1982). Its crystal structure consists of isolated Cs atoms and of chains of hydrogen-bonded selenate ions (Baran & Lis, 1987).

The crystal growth of $N(CH_3)_4HSO_4$ could be improved to obtain an ordered phase at room temperature: the crystal growth in the presence of an external electric field could perhaps solve the problem. Such a field may favor the presence of a unique orientation for the SO_4 tetrahedra.

We would like to thank H. Berger for his invaluable help with crystal growing, Dr J. P. Rivera for the optical measurements and Professor H. Arend for supplying some crystals and DSC measurements. We wish to thank Dr Kurt Schenk for valuable discussions and suggestions. This work was partially supported by Conselho Nacional de Densenvolvimento Cientifico e Tecnolólico (CNPq-Brazil).

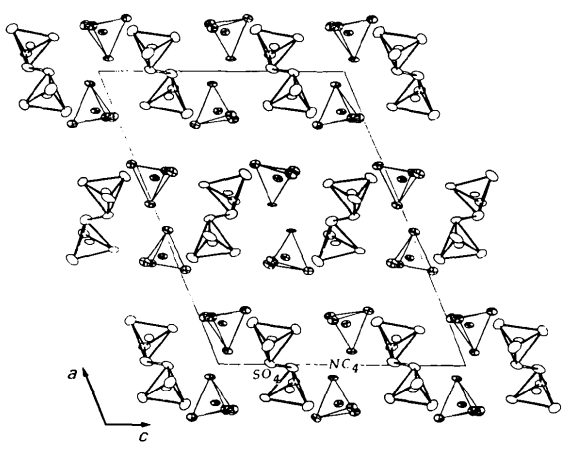

Fig. 7. Projection along [010] of the structure of the LT (ordered) phase of TMSO, corresponding to one of the twin domains.

References

AREND, H. (1984). Private communication.

AREND, H., PERRET, R., WUEST, H. & KERKOC, P. (1986). *J. Cryst. Growth*, **74**, 321–325.

BARAN, J. & LIS, T. (1987). *Acta Cryst.* C**43**, 811–813.

BARANOV, A. I., SHUVALOV, L. A. & SHCHAGINA, N. M. (1982). *JETP Lett.* **36**, 459–462.

BLINC, R., LAHAJNAR, G., ZUPANCIČ, I. & AREND, H. (1984). *Solid State Commun.* **51**, 751–752.

CROMER, D. & MANN, J. B. (1968). *Acta Cryst.* A**24**, 321–324.

DIDISHEIM, J.-J. & SCHWARZENBACH, D. (1987). *Acta Cryst.* A**43**, 226–232.

HAMILTON, W. C. & IBERS, J. A. (1968). *Hydrogen Bonds in Solids.* New York, Amsterdam: W. A. Benjamin.

ITOH, K., OZAKI, T. & NAKAMURA, E. (1981). *Acta Cryst.* B**37**, 1908–1909.

JOHNSON, C. K. (1965). *ORTEP.* Report ORNL-3794. Oak Ridge National Laboratory, Tennessee, USA.

RIVERA, J.-P., SPEZIALI, N. L., BERGER, H., AREND, H. & SCHMID, H. (1990). *Ferroelectrics*, **105**, 183–188.
SAWADA, S., YAMAGUCHI, T. & SUZUKI, H. (1985). *Ferroelectrics*, **63**, 3–11.
SIMMONS, E. H. & HEINE, V. (1987). *Acta Cryst.* A**43**, 626–635.
SPEZIALI, N. L. (1989). *Phase Transitions in* Cs_2CdBr_4 *and* $N(CH_3)_4HSO_4$: *a Crystallographic Study of Normal and Modulated Phases*. PhD Thesis, Univ. of Lausanne, Switzerland.
STEWART, J. M., KUNDELL, F. A. & BALDWIN, J. C. (1972). The *XRAY*72 system. Tech. Rep. TR-192. Computer Science Center, Univ. of Maryland, College Park, Maryland, USA. Modified by D. SCHWARZENBACH.
STEWART, R. F., DAVIDSON, E. R. & SIMPSON, W. T. (1965). *J. Chem. Phys.* **42**, 3175–3187.
WOLFF, P. M. DE, JANSSEN, T. & JANNER, A. (1981). *Acta Cryst.* A**37**, 625–636.
YAMAMOTO, A. (1982). *Acta Cryst.* A**38**, 87–92.

Acta Cryst. (1991). B**47**, 766–771

Determination of the Structure of Papaya Protease Omega

BY RICHARD W. PICKERSGILL*

Protein Engineering Department, AFRC Institute of Food Research, Reading Laboratory, Shinfield, Reading, Berkshire RG2 9AT, England

PIERRE RIZKALLAH

SERC Daresbury Laboratory, Daresbury, Warrington WA4 4AD, England

AND GILLIAN W. HARRIS AND PETER W. GOODENOUGH

Protein Engineering Department, AFRC Institute of Food Research, Reading Laboratory, Shinfield, Reading, Berkshire RG2 9AT, England

(*Received* 13 *September* 1990; *accepted* 11 *March* 1991)

Abstract

The structure of papaya protease omega (ppΩ) has been determined using Enraf–Nonius FAST TV data collected using the Daresbury Synchrotron Radiation Source (SRS). This is the first protein structure to be determined using the FAST/SRS combination and the first protein structure to be solved in space group $P3_112$. The structure has been refined to a crystallographic R factor of 0·1549 for all data in the range 10·0–1·8 Å.

1. Introduction

Papaya protease omega (ppΩ) is a cysteine protease from the latex of *Carica papaya*. ppΩ is homologous to papain (69% sequence identity; Dubois, Kleinschnidt, Schnek, Looze & Braunstzen, 1988) and the level of homology suggests that the structures of papain and ppΩ are similar and that the structure of ppΩ may therefore be solved by molecular replacement. The structure of papain was determined by multiple-isomorphous replacement and refined by Drenth and colleagues (Kamphuis, Kalk, Swarte & Drenth, 1984). A monoclinic ($P2_1$) crystal form has been solved by molecular replacement recently (Pickersgill, Harris & Garman, 1991) and refined to $R = 0{\cdot}1596$ using 10·0 to 1·60 Å data. This structure was used as the search model in molecular replacement.

The activity of ppΩ is similar to that of papain although subtle differences in specificity and stability have been reported.

ppΩ crystals diffract only weakly using a sealed-tube source and to a resolution limit of about 2·6 Å using X-rays from a rotating-anode source. At the Daresbury synchrotron radiation source (SRS) these crystals diffracted to 1·8 Å. This paper reports data collection, reduction and the use of these data to solve and refine the structure of ppΩ.

2. Experimental procedures

2.1. *Crystals and SRS/FAST data collection and reduction*

Protease Ω was eluted from a carboxymethyl-Sepharose column and dialysed against 100 mM sodium acetate at pH 5·0 containing 2·0 mM mercuric chloride (Pickersgill, Sumner & Goodenough, 1990). The mercuric chloride prevented autolysis of the protein. Before crystallization the protein was dialysed against 50 mM Tris buffer at pH 8·0 containing 250 mM sodium chloride to remove any

* Author to whom correspondence should be addressed.

0108-7681/91/050766-06$03.00